J. Min. Metall. Sect. B-Metall. 59 (1) (2023) 1 - 15

Journal of Mining and Metallurgy, Section B: Metallurgy

RECENT ADVANCES OF THE THERMODYNAMIC BEHAVIOR OF TIN SPECIES IN AQUEOUS SOLUTION

D.-R. Yang [a,b], Z.-L. Wu [c,d], K. Ren [a,b], P. Dong [a,b], D. Zhang [a,b *], B. Yang [a,b], F. Liang [a,b *]

[a] Faculty of Metallurgical and Energy Engineering, Kunming University of Science and Technology, Kunming, China

[b] National Engineering Research Center for Vacuum Metallurgy, Kunming University of Science and Technology, Kunming, China

[c] College of Materials Science and Engineering, Shenzhen University, Shenzhen, China

[d] Zhejiang LAMP Co., Ltd., Wenzhou, China

(Received 17 June 2022; Accepted 21 November 2022)

Abstract

Thermodynamic behavior has been extensively used to evaluate the stability of materials and predict the direction of the chemical reaction at different pH values, temperatures, potentials, and ion concentrations. Although researching efforts on Sn species in an aqueous solution system (Sn/H_2O) of acid, alkali, and salt have been reported, scattered data leads to the inefficiency of a thermodynamic method in the practical application. This article provides a brief review on the potential-pH diagram for Sn/H_2O system, which reflects the thermodynamic behavior of Sn species in an aqueous solution and extracts thermodynamic data for the practical application of Sn species. Firstly, the relationship of the thermodynamic behavior, potential-pH diagram, and equilibrium relations of Sn species for Sn/H_2O system was overviewed. Additionally, the potential-pH diagram of Sn/H_2O system at different temperatures (298 K, 373 K, and 550 K), dissolved Sn activities (1, 10^{-1}, 10^{-3}, and 10^{-6}), and the potential-pH diagram of the Sn species in a chloridion aqueous solution (Sn/H_2O-Cl) was summarized. Finally, the application prospect of the potential-pH diagram for Sn/H_2O system was investigated in the intelligent simulation of Sn metallurgy and the practical application of Sn materials.

Keywords: *Sn/H_2O system; Potential-pH diagrams; Thermodynamic behavior; Redox potential; Equilibrium*

1. Introduction

Sn(Tin)-based materials have received extensive applications in the fields of the electronic technology, communications engineering, chemistry, machinery, and aerospace industry owing to its low melting point, strong exhibition, strong plasticity, corrosion protection, and other excellent characteristics. Moreover, the novel Sn-based materials such as refractory materials, special glasses, and battery materials have brought a wide application prospect for Sn-based materials [1].

Sn/H_2O system is widely used in the hydrometallurgy [2], electroplating [3], organotin chemistry [4], and the production process of Sn products. Therefore, the thermodynamic data of the transformation of Sn species in the system plays an important role in studying thermodynamic behaviors. Fortunately, the potential-pH (φ-pH) diagram for Sn/H_2O system provides an intuitive way to judge the potential-pH domain in which each species is stable [5-7]. It also can be used to determine the direction of the chemical reaction and explain thermodynamic behaviors of Sn/H_2O system to optimize the production process [8, 9]. Therefore, the φ-pH diagram of Sn/H_2O system can provide a theoretical guidance for the produce process and the application of Sn to meet the electrochemical energy storage and catalytic fields. However, Sn compounds with different oxidation states have different thermodynamic behaviors, leading to the formation of complex compounds in various systems, which makes it difficult to obtain the complete thermodynamic data.

In this review, the development of the φ-pH diagram of Sn/H_2O system is discussed. The thermodynamic behavior of Sn/H_2O system with different temperatures and ionic concentrations are summarized in detail. Additionally, the information on the application of φ-pH diagrams for optimizing the production processes is overviewed. Finally, the perspective and suggestion about the development of the φ-pH diagram of Sn/H_2O are presented.

**Corresponding author: liangfeng@kust.edu.cn*

https://doi.org/10.2298/JMMB220617001Y

2. Thermodynamic and potential-pH diagram method

Since the 1920s, the relationship between the redox potential and the pH value has been extensively reported, and then Clark was the first to use it to describe the relationship of the electrochemical equilibrium between the water molecule and the hydrogen ion or oxygen. After that, it was used to determine the equilibrium potential and pH value of systems with the coexistence of oxidants or reductants [10]. In the 1930s, Pourbaix developed the above theory and further improved the φ-pH diagram. Then Pourbaix's group optimized a φ-pH diagram and determined the relationship between a pH value and a reaction potential of ions and solid compounds in solution by using thermodynamic parameters [11]. Based on this, the relationship between the reaction potential and pH value was deduced from the reaction components, and the thermodynamic diagram with the redox potential as an ordinate and the pH value as an abscissa was obtained.

According to the effect of the reaction potential and pH value on the thermodynamic behavior with the different temperatures and activities of components, the φ-pH diagram was constructed [12, 13]. The lines in the φ-pH diagram correspond to a thermodynamic-equilibrium equation, and the points of intersection for lines represent the equilibrium under the same potential and pH. Additionally, the area between lines in a φ-pH diagram indicates the thermodynamic stability region of species. Moreover, two types of the φ-pH diagram, the planar diagram and three-dimensional diagram, have been reported, and the planar potential-pH diagram will be described in this paper [10, 14].

In short, the thermodynamic behavior for Sn/H_2O system is largely dependent on pH, temperature, equilibrium constant, potential, and ion concentration [15]. The transformation level and the stability of Sn species in an aqueous solution might be distinctly expressed by the free energy ($\Delta_r G_m^{\Theta}$/kJ·mol^{-1}) [16] and the equilibrium constant (K^{Θ}) [17], which is derived from the thermodynamic theory [18] and the dynamics theory of a solution [19].

2.1. Influence of pH on Sn behavior in an aqueous solution

The dissociative behavior for an aqueous solution might be expressed by $H_2O = H^+ + OH^-$, where the expression of equilibrium constant (K^{Θ}) was obtained at 298 K as follows (α is the activity of the species) [20].

$$K^{\theta} = \left[H^+\right] \cdot \left[OH^-\right] = \alpha_{(H^+)} \cdot \alpha_{(OH^-)} = 1.0 \cdot 10^{-14} \quad (1)$$

$$pH - log\alpha_{(OH^-)} = 14 \quad (2)$$

However, the ionization and solubility of compounds in an aqueous solution varied with the pH value and the free energy [21, 22]. Sn(II) ion, for example, the dissociation equilibrium of $Sn(OH)_2$ in Sn/H_2O system might be expressed by $Sn(OH)_2(s) = Sn^{2+} + 2OH^-$. According to the theory of the chemical equilibrium, the standard thermodynamic-equilibrium constant is given by $K^{\Theta} = \alpha_{(Sn^{2+})} \cdot (\alpha_{(OH^-)})^2 / \alpha(Sn(OH)_2(s))$ and simplified into $K^{\Theta} = \alpha_{(Sn^{2+})} \cdot (\alpha_{(OH^-)})^2$. While the activity of $\alpha(Sn(OH)_2(s))$ is 1, the following logarithmic expression can be obtained.

$$logK^{\theta} = log\alpha_{(Sn^{2+})} + 2log\alpha_{(OH^-)} \quad (3)$$

The variation of $\Delta_r G_m^{\Theta}$ (kJ·mol^{-1}) for this reaction was a characteristic constant for the process from $\Delta_r G_m^{\Theta} = -RTlnK^{\Theta}$, where K^{Θ} is the equilibrium constant. Meanwhile, the relationship between the activity of Sn^{2+} and OH^- was obtained as follows:

$$log\alpha_{(Sn^{2+})} = -\Delta_r G_m^{\theta} / (2.303RT) - 2log\alpha_{(OH^-)} \quad (4)$$

Where R is the molar gas constant (8.314 J·mol^{-1}·K^{-1}), T is the absolute temperature (K), and $\alpha_{(Sn^{2+})}$ is the activity of Sn^{2+}.

The relationship between the pH and the ion activity at 298 K is given by the following equation.

$$pH = 14 - \Delta_r G_m^{\theta} / (5705.85 \cdot 2) - 0.5log\alpha_{(Sn^{2+})} \quad (5)$$

Taking $Sn(OH)_2$ in Sn/H_2O system as an example, a reaction in which H^+ ions were involved but not involved in redox reaction, these equilibriums depended on the pH but not on the redox potential. It is represented by a set of vertical lines in the φ-pH diagram where pH and potential are the x-coordinate and y-coordinate, respectively. Remarkably, the solubility of $Sn(OH)_2$ in an aqueous solution varied with pH, while the concentration of Sn^{2+} and OH^- in pure water could be ignored, so the activity coefficient of Sn^{2+} and OH^- in pure water was 1.

2.2. Influence of the redox potential on Sn behavior in an aqueous solution

According to the electrochemical reaction theory, the redox reaction involves the transfer of electrons at the interface between an electrical conductor and an ionic conductor. It can be defined as two half-cell reactions, including the oxidation and reduction processes [19]. Specifically, the oxidation reaction occurs on the anodic surface, while the reduction reaction occurs on the cathodic surface according to the reversible equilibriums (6) ~ (8).

$$Sn + 2H^+ = Sn^{2+} + H_2 \quad (6)$$

$$Oxidation\ reaction:\ Sn^{2+} + 2e = Sn \quad (7)$$

$$Reduction\ reaction: 2H^+ + 2e = H_2 \quad (8)$$

2.2.1. Redox potential (φ^{θ}) of Sn ion and metal

The reaction that metallic Sn forms into Sn^{2+} in Sn/H_2O system is represented as the equation (7). The relationship between the redox potential and the ion activity of the above reaction in an aqueous solution can be expressed by the Nernst equation (9) [23].

$$\varphi = \varphi^{\theta}_{(Sn^{2+}/Sn)} + (RT/zF)\cdot ln\alpha_{(Sn^{2+})} \quad (9)$$

Where z represents the electron transfer coefficient during a redox reaction, F represents the Faraday constant (96500 C·mol^{-1}), and φ^{Θ} represents the standard redox potential (V). The relationship between $\Delta_r G_m^{\Theta}$ and φ^{Θ} [24] is given by equations (10) ~ (12).

$$\Delta_r G_m^{\theta} = -zF\varphi^{\theta}_{(Sn^{2+}/Sn)} \quad (10)$$

$$\varphi^{\theta}_{(Sn^{2+}/Sn)} = -\Delta_r G_m^{\theta}/(96500\cdot z) \quad (11)$$

$$\varphi = -\Delta_r G_m^{\theta}/(96500\cdot z) + (RT/zF)\cdot ln\alpha_{(Sn^{2+})} \quad (12)$$

Taking Sn^{2+} in Sn/H_2O system as an example, a reaction in which H^+ ions were not involved but they were involved in oxidation state change (equation (7)), these equilibriums depended on the redox potential, but not on the pH value. This was represented by a set of horizontal lines in a φ-pH diagram. The location of the lines was related to the value of the logarithm of the Sn^{2+} activities (e.g., $ln_{(Sn^{2+})}$).

2.2.2. Redox potential of the conversion from Sn(II) to Sn(IV)

The conversion from Sn(II) to Sn(IV) is shown in the equation (13). Redox potentials in the equations (14) and (15) are in conformity with the Nernst equation.

$$Sn^{4+} + 2e = Sn^{2+} \quad (13)$$

$$\varphi_{(Sn^{4+}/Sn^{2+})} = \varphi^{\theta}_{(Sn^{4+}/Sn^{2+})} + (RT/zF)\cdot ln(\alpha_{(Sn^{4+})}/\alpha_{(Sn^{2+})}) \quad (14)$$

$$\varphi = -\Delta_r G^{\theta}/(96500\cdot z) + (RT/zF)\cdot (ln\alpha_{(Sn^{4+})} - ln\alpha_{(Sn^{2+})}) \quad (15)$$

Taking the conversion from Sn(II) to Sn(IV) in Sn/H_2O system as an example, a reaction in which H^+ ions were not involved but were involved in oxidation state change(equation (9)), these equilibriums depended on the redox potential, but not on the pH value. This was represented by a set of a horizontal line in a φ-pH diagram. The location of the lines was related to the value of the logarithm of the $ln\alpha_{(Sn^{2+})}$ and $ln\alpha_{(Sn^{4+})}$.

2.2.3. Redox potential of the complexation reaction for Sn(II) and Sn(IV)

Thermodynamic behavior for the Sn(II) and Sn(IV) compounds in an aqueous solution extensively depend on a pH value [25] and a coexisting anion. Previous reports indicated that Sn(II) compounds mainly existed in insoluble or soluble salts with pH < 7, while Sn(II) and Sn(IV) compounds were readily hydrolyzed in an aqueous solution to form oxide hydrates, which were then dissolved in acid or alkali solutions and existed as $[Sn(OH)_3]^-$ [26]. The reaction equilibrium of Sn(II) and Sn(IV) ions is shown in the expressions (16) and (17) [27]. The thermodynamic equilibriums of $Sn(OH)_2$ are given by the equations (18) and (19) and the expression of the redox potential change is given by the below equations (20):

$$xSn^{2+} + yH_2O = Sn_x\left[(OH)_y\right]^{(2x-y)+} + yH^+ \quad (16)$$

$$Sn^{4+} + yH_2O = Sn\left[(OH)_y\right]^{(4-y)+} + yH^+ \quad (17)$$

$$Sn^{2+} + 2OH^- = Sn(OH)_2(s) \quad (18)$$

$$Sn(OH)_2(s) + 2e = Sn + 2OH^- \quad (19)$$

$$\varphi_{(Sn(OH)_2/Sn)} = \varphi^{\theta}_{(Sn(OH)_2/Sn)} - (RT/zF)\cdot ln(\alpha_{(OH^-)})^2 \quad (20)$$

Taking the conversion from $Sn(OH)_2$ to Sn in Sn/H_2O system as an example, a reaction in which H^+ ions and change of oxidation state were involved (equation (19)), the direction, and the equilibrium of the reaction depended on the redox potential and the pH value. This was represented by a set of oblique parallel lines in a φ-pH diagram. The location of the lines was related to the value of the logarithm of the function of pH value and Sn^{2+} activities.

3. Thermodynamic equilibriums of Sn in an aqueous solution

Owing to the formation of Sn oxide layer to prevent it from contacting active substances, metallic Sn displayed the excellent stability in air, but it was facially dissolved in a strong acid and alkaline solution [28, 29]. Sn is a polyvalent metal with the valence of Sn(II), Sn(Ш), Sn(IV), but Sn(II) and Sn(IV) are common in previous studies [30]. Among them, Sn(II) and Sn(IV) ions in an aqueous solution are hydrolyzed in an aqueous solution to form a hydrated oxide [31, 32]. Davies [32] found that Sn(II) and Sn(IV) species showed different oxides or hydroxyl compounds in different pH values. For example, Sn(II) and Sn(IV) were converted to a hydrated oxide precipitation in

systems with pH > 2.5. However, sodium stannate (Sn(IV)) was stable in an alkaline system, whereas stannite (Sn(II)) formed into metallic Sn in an alkaline system. The conversion sequence of Sn was Sn → Sn(II) → Sn(IV) in an alkaline system, while the conversion sequence of Sn was Sn → $[Sn(OH)_3]^-$ → $[Sn(OH)_6]^{2-}$ in an acidic system [29]. Drogowska [33] found that Sn(IV) species were mainly $[SnO(OH)_3]^-$ (pH ≥ 8) and $SnO(OH)_2$ (pH < 7), and moreover $Sn(OH)_2$ was the main compound of Sn(II) species in natural water. Pourbaix summarized the free energy for Sn compounds ($[HSnO_2]^-$, $[SnO_3]^{2-}$, SnO, SnO_2, and SnH_4(g)) by the electrochemical corrosion theory [34]. It helpfully provided for many thermodynamic references to the Sn production and application process. Kragten et al. investigated the dissolution behavior for the Sn(IV) compounds in an aqueous solution and indicated that Sn(IV) formed insoluble $SnO_2{\cdot}nH_2O$ in a strong acidic condition. They confirmed that Sn(IV) species in an aqueous solution conformed to the following chemical changes: Sn^{4+} ↔ $Sn(OH)^{3+}$ ↔ $[Sn(OH)_2]^{2+}$ ↔ $[Sn(OH)_3]^+$ ↔ $Sn(OH)_4$ ↔ $[Sn(OH)_5]^-$ ↔ $[Sn(OH)_6]^{2-}$ and $Sn(OH)_4$ ↔ $SnO_2{\cdot}nH_2O$ [35]. Begum found that Sn reacted with halogen to form the $Sn(OH)_2$ passivation layer on the metallic Sn surface in a solution of sodium hydroxide, but the passivation layer was oxidized to SnO_2 at a higher redox potential [36]. Thermodynamic behavior of Sn(II) has also been widely discussed in previous studies, such as $SnOH^+$, $Sn(OH)_{2ads}$, $[Sn(OH)_3]^-$, $[Sn_2(OH)_2]^{2+}$, and $[Sn_3(OH)_4]^{2+}$ [37]. Din et al summarized a set of $\Delta_rG_m^\Theta$ and φ^Θ data by investigating the reaction of Sn anode in alkaline solution, and they found that the primary passivity was attained in all solutions when the metal was covered with a film of $Sn(OH)_2$ or SnO [38].

3.1. Potential-pH diagram for water

Sn species in an aqueous solution could be indispensable to the fields of the metal corrosion [39], metallurgy [40], analytical chemistry [41], and electrochemical industry [42]. However, aqueous solution dissociates producing oxygen when the potential is above its redox potential, and aqueous solution dissociates release hydrogen when the potential is below its redox potential [43, 44]. In a system which aqueous solution participates in redox reactions, all aqueous chemistry would have to happen in the thermodynamic stability field. On the contrary, chemical reactions may happen outside of the water stability field without an aqueous solution [45]. Obviously, the thermodynamic stability of water would affect the behavior of Sn/H_2O system, which is the reason why the thermodynamic behavior of water is chosen for the potential-pH diagram theory of Sn/H_2O system. As shown in Figure 1, the region below the line b in Figure 1a was defined by the equation (24), where hydrogen was precipitated from the solution by the equation (21). The figures were drawn by the OriginLab software of 2019b version, all of which were drawn by the same software. In contrast, the region above the line a was defined by the equation (28), where oxygen was precipitated from the solution by the equation (25) [46].

At 298 K, the Nernst equation was used to calculate the relationship of potential, pH value, and hydrogen partial pressure, which were expressed by two equilibrium equations (23) and (24) [45], where $p_{(H_2)}$ was the hydrogen partial pressure (Pa), and p^Θ was the standard atmospheric pressure (Pa). Below the line b, the redox potential was more negative than hydrogen, resulting in the generation of hydrogen (Figure1a).

$$2H^+ + 2e = H_2 \tag{21}$$

$$2H_2O + 2e = H_2 + 2OH^- \tag{22}$$

$$\varphi_{(H_2O/H_2)} = \varphi_{(H^+/H_2)} = \varphi^\theta{}_{(H^+/H_2)} + (RT/zF)\cdot ln((\alpha_{(H^+)})^2 / (p_{(H_2)} / p^\theta)) \tag{23}$$

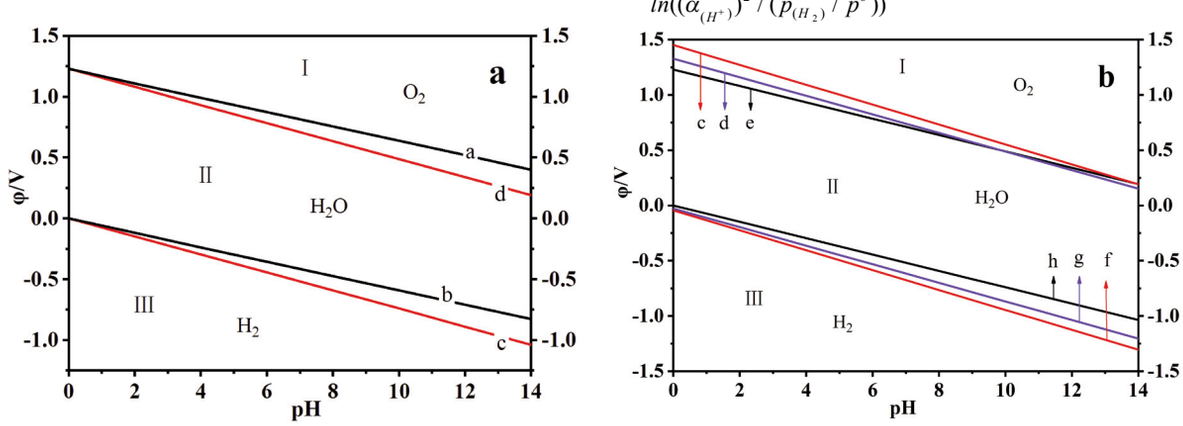

Figure 1. a *The φ-pH diagram for water with* $p_{(O_2)} = p_{(H_2)} = p^\Theta$, *lines a and b corresponding to 298 K, Lines c and d corresponding to 373 K [5].* ***b*** *The φ-pH diagram for water under saturated vapor pressure, lines c and f corresponding to 398 K, lines e and h corresponding to 448 K, and lines d and g corresponding to 478 K [5]*

$$\varphi_{(H^+/H_2)} = -0.059pH - 0.0295log(p_{(H_2)}/p^{\theta}) \quad (24)$$

The oxygen evolution reaction is usually defined by the equations (25) and (26). According to the expressions of (27) and (28) [45], where $p_{(O_2)}$ was the oxygen partial pressure (Pa), the relationship of potential, pH value, and hydrogen partial pressure at 298 K was calculated. In the area above the line a in Figure 1a, the thermodynamic properties of water were unstable.

$$O_2 + 4H^+ + 4e = 2H_2O \quad (25)$$

$$4OH^- + 4e = O_2 + 2H_2O \quad (26)$$

$$\varphi_{(O_2/H_2O)} = \varphi_{(O_2/OH^-)} = \varphi^{\theta}{}_{(O_2/OH^-)} + (RT/zF)\cdot ln((p_{(O_2)}/p^{\theta})\cdot(\alpha_{(H^+)})^4) \quad (27)$$

$$\varphi_{(O_2/OH^-)} = 1.229 - 0.0591pH + 0.0148log(p_{(O_2)}/p^{\theta}) \quad (28)$$

The region between the line a and line b belonged to the thermodynamically stable region of water (Figure 1a).

As shown in Figure 1b, lines c and f, lines e and h, and lines d and g represented the potential-pH diagram for water at the saturated vapor pressure of 398 K, 448 K, and 478 K, respectively. Similarly, the region between two lines belonged to the thermodynamically stable region of water. Lines c and f, lines e and h, lines d and g conformed to the equations (23) and (27), which supplemented the thermodynamic data of water at a high temperature.

3.2. Potential-pH diagram for Sn/H_2O system

Since Sn(II) and Sn(IV) compounds are intersex ions, Sn(IV) compounds are acidic in an aqueous solution, and Sn/H_2O systems are extremely complex [32]. The standard free energy of formation (G_f^{θ}/kJ·mol^{-1}) for the selected Sn compounds at 373 K and 550 K are shown in Figure 2, whose thermodynamic data was obtained from the reported literature [27, 34, 47].

The thermodynamic behavior of the reaction components was derived directly from the Nernst equation, and the influence of pH on the stability of components was derived from K^{Θ} and ΔG_f^{Θ}. The possible chemical equilibrium and thermodynamic data of Sn/H_2O system are shown in Table 1.

The φ-pH diagram for Sn/H_2O system in Figure 3 was derived from the relationship of the potential, pH value, and equilibrium that were provided by the logarithm of the gas partial pressure and the concentration function of Sn compounds in Table 1. This provided the information that Sn and SnH_4(g) (p(SnH_4(g) were the SnH_4(g) partial pressure (Pa)) and were thermodynamically stable in strongly reducing systems, whereas Sn(II) compounds were pH-dependent. Furthermore, it clearly indicated that metallic Sn may be oxidized to SnO_2 at a redox potential of about 2.02 V (Figure 3c) and then form a passivation film with a limited range of a pH value and redox potential [58]. Sn(II) ion was unstable in a wide pH range (0 ~ 14), indicating that Sn(II) compounds were in the form of Sn^{2+}, $SnOH^+$, $Sn(OH)_2$, $[HSnO_2]^-$, and $[Sn(OH)_3]^-$. At the higher redox potential, stannous was oxidized to stannic species, and the main Sn(IV) existing in the higher redox potential was SnO_2(s), $Sn(OH)_4$, $[SnO_3]^{2-}$, and $[Sn(OH)_6]^{2-}$ (Figure 3c).

Under certain conditions of pH, the redox potential, ionic concentration, and Sn species were stable in a Sn/H_2O system until the original equilibrium was broken. As shown in Figure 3, Sn may corrode in an aqueous solution with the condition change. However, Sn was stable in the φ-pH diagram region, because Sn surface was covered by $Sn(OH)_2$(s), $Sn(OH)_4$(s), SnO(s), and SnO_2(s), resulting in a decrease in the dissolution rate of metal Sn.

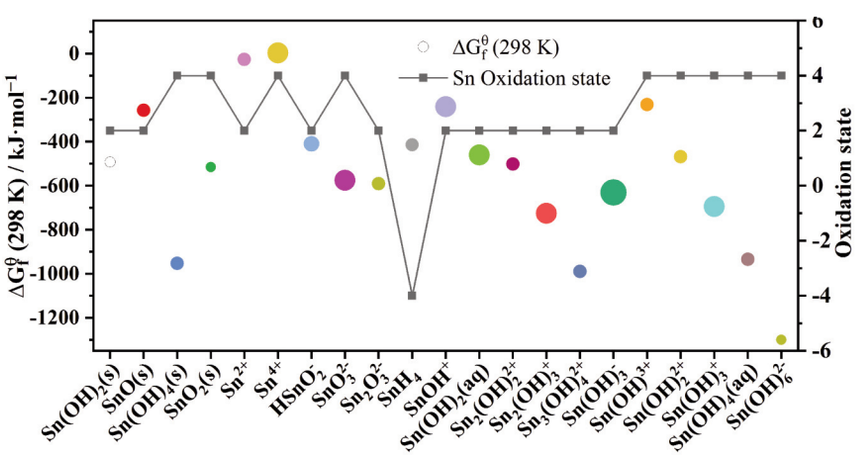

Figure 2 *Schematic illustration of the selected ΔG_f^{Θ} for Sn/H_2O system at 298 K. The Sn species data were retrieved from the references [27, 34, and 47]*

Table 1. *The reaction equilibrium for Sn/H_2O system at 298 K*

Equilibrium [Ref.]	φ / (V) or pH
$Sn^{2+} + 2e = Sn$, [34, 48, 49, 50]	$\varphi = -0.14 + 0.029\log\alpha_{(Sn^{2+})}$
$Sn^{4+} + 2e = Sn^{2+}$, [34, 48]	$\varphi = 0.15 + 0.029\log(\alpha_{(Sn^{4+})}/\alpha_{(Sn^{2+})})$
$SnO + 2H^+ = Sn^{2+} + H_2O$, [34, 47]	$pH = 0.52 - 0.5\log\alpha_{(Sn^{2+})}$
$SnO_2 + 4H^+ = Sn^{4+} + 2H_2O$, [34]	$pH = -1.94 - 0.25\log\alpha_{(Sn^{4+})}$
$SnO + H_2O = H^+ + [HSnO_2]^-$, [34, 47, 50, 51]	$pH = 14.78 + \log\alpha_{[HSnO_2]^-}$
$SnO + 2H^+ + 2e = Sn + H_2O$, [34]	$\varphi = -0.11 - 0.059pH$
$[HSnO_2]^- + 3H^+ + 2e = Sn + 2H_2O$, [34]	$\varphi = 0.33 - 0.089pH + 0.029\log\alpha_{[HSnO_2]^-}$
$Sn + 4H^+ + 4e = SnH_4$, [34]	$\varphi = 1.074 - 0.059pH - 0.015\log p_{(SnH_4)}$
$Sn(OH)_2 = Sn^{2+} + 2OH^-$, [47]	$pH = 0.71 - 0.5\log\alpha_{(Sn^{2+})}$
$Sn(OH)_4 + 4H^+ = Sn^{4+} + 4H_2O$, [27]	$pH = -0.29 - 0.25\log\alpha_{(Sn^{4+})}$
$Sn(OH)_2 + 2e = Sn + 2OH^-$, [42, 44, 52]	$\varphi = -0.094 - 0.059pH$
$Sn(OH)_4 + 2e = Sn(OH)_2 + 2OH^-$, [36, 53, 54]	$\varphi = 0.073 - 0.059pH$
$Sn(OH)_4 + 2e = Sn^{2+} + 4OH^-$, [35]	$\varphi = 0.12 - 0.12pH - 0.029\log\alpha_{(Sn^{2+})}$
$Sn(OH)_2 = H^+ + [HSnO_2]^-$, [47]	$pH = 14.39 + \log\alpha_{[HSnO_2]^-}$
$Sn(OH)_4 + 2OH^- = [Sn(OH)_6]^{2-}$, [48]	$pH = 11.09 + 0.5\log\alpha_{[Sn(OH)_6]^{2-}}$
$[Sn(OH)_6]^{2-} + 2e = Sn(OH)_2 + 4OH^-$, [48]	$\varphi = 0.73 - 0.12pH + 0.029\log\alpha_{[Sn(OH)_6]^{2-}}$
$[Sn(OH)_6]^{2-} + 2e = [HSnO_2]^- + H_2O + 3OH^-$, [48]	$\varphi = 0.31 - 0.089pH + 0.029\log(\alpha_{[Sn(OH)_6]^{2-}}/\alpha_{[HSnO_2]^-})$
$SnO_2 + 4H^+ + 2e = Sn^{2+} + 2H_2O$, [34]	$\varphi = -0.077 - 0.12pH - 0.029\log\alpha_{S(Sn^{2+})}$
$Sn(OH)_4 + 2e = SnO + 2OH^- + H_2O$, [48, 54]	$\varphi = 0.085 - 0.059pH$
$[Sn(OH)_6]^{2-} + 2e = SnO + H_2O + 4OH^-$, [48]	$\varphi = 0.74 - 0.12pH + 0.029\log\alpha_{[Sn(OH)_6]^{2-}}$
$[Sn(OH)_6]^{2-} = SnO_2 + 2H_2O + 2OH^-$, [48]	$pH = 14.38 + 0.5\log\alpha_{[Sn(OH)_6]^{2-}}$
$[SnO_3]^{2-} + 3H^+ + 2e = [HSnO_2]^- + H_2O$, [34]	$\varphi = 0.37 - 0.089pH + 0.029\log(\alpha_{[SnO_3]^{2-}}/\alpha_{[HSnO_2]^-})$
$SnO_2 + H_2O = 2H^+ + [SnO_3]^{2-}$, [34]	$pH = 15.55 + 0.5\log\alpha_{[SnO_3]^{2-}}$
$SnO_2 + H_2O + 2e = [HSnO_2]^- + OH^-$, [48]	$\varphi = -0.59 - 0.029pH - 0.029\log\alpha_{[HSnO_2]^-}$
$Sn^{2+} + H_2O = SnOH^+ + H^+$, [55, 56, 57]	$pH = 3.88 + \log(\alpha_{Sn(OH)^+}/\alpha_{(Sn^{2+})})$
$Sn^{2+} + 3H_2O = [Sn(OH)_3]^- + 3H^+$, [55, 56]	$pH = 6.24 + 0.33\log\alpha_{[Sn(OH)_3]^-}/\alpha_{(Sn^{2+})}$
$2Sn^{2+} + 2H_2O = [Sn_2(OH)_2]^{2+} + 2H^+$, [55, 57]	$pH = 2.19 + 0.5\log\alpha_{[Sn2(OH)_2]^{2+}} - \log\alpha_{Sn^{2+}}$
$2Sn^{2+} + 3H_2O = [Sn_2(OH)_3]^+ + 3H^+$, [55]	$pH = 2.25 + 0.33\log\alpha_{[Sn2(OH)_3]^+} - 0.67\log\alpha_{(Sn^{2+})}$
$3Sn^{2+} + 4H_2O = [Sn_3(OH)_4]^{2+} + 4H^+$, [55, 57]	$pH = 1.66 + 0.25\log\alpha_{[Sn3(OH)_4]^{2+}} - 0.75\log\alpha_{(Sn^{2+})}$
$[SnO_3]^{2-} + 3H^+ + 2e = [Sn(OH)_3]^-$, [55]	$\varphi = 0.287 - 0.089pH + 0.029\log(\alpha_{[SnO_3]^{2-}}/\alpha_{[Sn(OH)_3]^-})$
$Sn^{4+} + 3H_2O = [SnO_3]^{2-} + 6H^+$, [55]	$pH = 3.89 + 0.167\log(\alpha_{[SnO_3]^{2-}}/\alpha_{S(Sn^{4+})})$

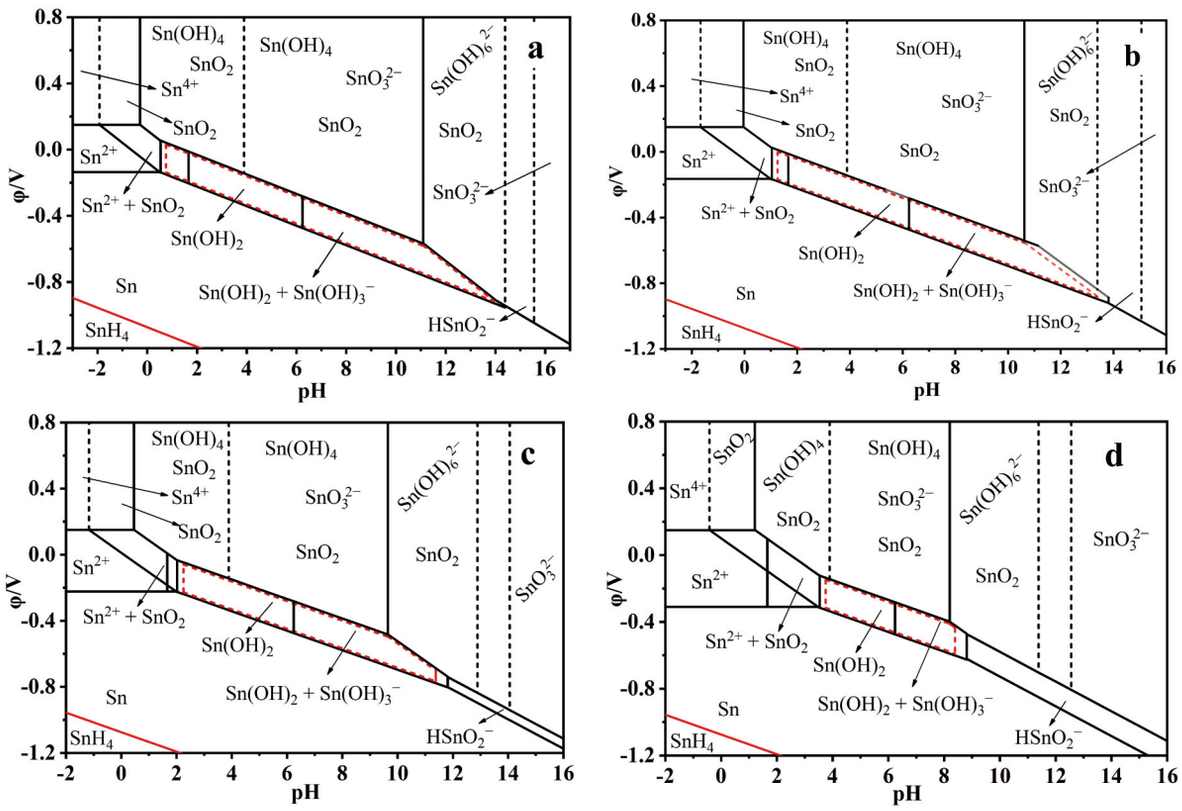

Figure 3. *Potential-pH diagrams for Sn/H_2O system at 298 K (p[SnH_4(g)] = p(H_2) = p^{Θ}) at the activity of dissolved Sn of* ***a*** *1,* ***b*** *10^{-1},* ***c*** *10^{-3}, and* ***d*** *10^{-6}. The Sn species data were retrieved from the reference [27, 34-36, 42, 44, 47-57]*

3.3. Potential-pH diagram for Sn/H_2O-anion complex systems

In a Sn/H_2O system, Sn ions react with ligands to form coordination compounds. In this paper, the thermodynamic data of Sn(II) and Sn(IV) reacting with Cl^-, F^-, $[CO_3]^{2-}$, $[SO_4]^{2-}$, and $[PO_4]^{3-}$ was investigated. The dissociation constants (K_d) of Sn(II) and Sn(IV) at 298 K are listed in Table 2 where I represents the ionic strength.

Recently, Sn and halide ions in an aqueous solution have been extensively studied in the production and application of Sn owing to advantages of their conductivity, stability, and low coast [59-62]. For example, Cigala demonstrated that 60% of the inorganic Sn(II) in an chloridion aqueous solution was $SnCl_n$ and Sn(OH)Cl (pH < 4.5) [37]. Séby et al confirmed that the influence of chloride ions on Sn(II) species could be ignored under the condition of pH > 4, while Sn(II) hydrolysate predominated in a system with a higher pH value [55]. The thermodynamic equilibriums of Sn(II) and Sn(IV) reacting with chloridion were obtained by the following equations (29 ~ 34) [33, 63]:

$$[SnCl_{(n-1)}]^{(3-n)+} + Cl^- = [SnCl_n]^{(2-n)+} \quad (29)$$

$$SnOH^+ + nCl^- = [SnOHCl_n]^{(1-n)+} \quad (30)$$

$$SnO(s) + 2H^+ + 4Cl^- = [SnCl_4]^{2-} + H_2O \quad (31)$$

$$SnOHCl \cdot H_2O(s) + H^+ + 3Cl^- = [SnCl_4]^{2-} + 2H_2O \quad (32)$$

$$SnO_2(s) + 4H^+ + 6Cl^- = [SnCl_6]^{2-} + 2H_2O \quad (33)$$

$$Sn^{2+} + Cl^- + 2H_2O = SnOHCl \cdot H_2O(s) + H^+ \quad (34)$$

As shown in Figure 4, the φ-pH diagram of Sn/H_2O-Cl system showed that the dissolved activity of Sn and chloride ions was 10^{-3} and 1 and p[SnH_4(g)] = 1 at 298 K. The complexation reaction to form Sn(II) and Sn(IV) chloride complexes($[SnCl_4]^{2-}$, SnOHCl, et al.) reduced the predominance area of Sn [27]. Furthermore, Sn(IV) was converted to SnOHCl·H_2O(s) at pH < 1 and to $[SnCl_4]^{2-}$ at pH ≈ 3. In acidic solutions containing chloride ions, Sn(IV) species were dominated by $[SnCl_6]^{2-}$.

3.4. Potential-pH diagram for Sn/H_2O system at elevated temperature

Hydrometallurgy, corrosion, chemistry, and other engineering processes mostly involve an elevated temperature. Therefore, φ-pH diagrams at an elevated temperature play an important role in Sn/H_2O

Table 2. *Complex dissociation constants of inorganic Sn with ligands ions at 298 K*

Equilibrium [Ref.]	$\log K_d$	I (mol L^{-1})	Medium
$SnF^+ = Sn^{2+} + F^-$, [33, 45]	– 4.0	1	$NaClO_4$
$SnF_2 = Sn^{2+} + 2F^-$, [33, 45]	– 6.68	1	$NaClO_4$
$[SnF_3]^- = Sn^{2+} + 3F^-$, [33, 45]	– 9.5	1	$NaClO_4$
$SnCl^+ = Sn^{2+} + Cl^-$, [33, 45]	– 1.18 ± 0.01	3	$NaClO_4$
$SnCl_2 = Sn^{2+} + 2Cl^-$, [33, 45]	– 1.74 ± 0.02	3	$NaClO_4$
$[SnCl_3]^- = Sn^{2+} + 3Cl^-$, [33, 45]	– 1.67 ± 0.04	3	$NaClO_4$
$[SnCl_4]^{2-} = Sn^{2+} + 4Cl^-$, [33, 45]	– 2.27	4	H_2SO_4
$SnOHCl = SnOH^+ + Cl^-$, [33, 45]	– 1.04	3	$NaClO_4$
$SnCl^{3+} = Sn^{4+} + Cl^-$, [33, 45]	– 3.71 ± 0.03	5	$NaClO_4$
$[SnCl_2]^{2+} = Sn^{4+} + 2Cl^-$, [33, 45]	– 6.46 ± 0.02	5	$NaClO_4$
$[SnCl_3]^+ = Sn^{4+} + 3Cl^-$, [33, 45]	– 8.78 ± 0.02	5	$NaClO_4$
$SnCl_4 = Sn^{4+} + 4Cl^-$, [33, 45]	– 9.48 ± 0.09	5	$NaClO_4$
$[SnCl_5]^- = Sn^{4+} + 5Cl^-$, [33, 45]	– 11.23 ± 0.06	5	$NaClO_4$
$[SnCl_6]^{2-} = Sn^{4+} + 6Cl^-$, [33, 45]	– 12.40 ± 0.05	5	$NaClO_4$
$SnBr^+ = Sn^{2+} + Br^-$, [45]	– 0.74 ± 0.04	1	$NaClO_4$
$SnBr_2 = Sn^{2+} + 2Br^-$, [45]	– 0.90 ± 0.05	1	$NaClO_4$
$[SnBr_3]^- = Sn^{2+} + 3Br^-$, [45]	– 1.34	3	$NaClO_4$
$[SnBr_4]^{2-} = Sn^{2+} + 4Br^-$, [45]	– 0.40 ± 0.05	3	$NaClO_4$
$[SnBr_5]^{3-} = Sn^{2+} + 5Br^-$, [45]	– 2.40 ± 0.1	8	$NaClO_4$
$[SnBr_6]^{4-} = Sn^{2+} + 6Br^-$, [45]	– 2.30 ± 0.1	8	$NaClO_4$
$SnI^+ = Sn^{2+} + I^-$, [45]	– 0.70 ± 0.5	4	$NaClO_4$
$SnI_2 = Sn^{2+} + 2I^-$, [45]	– 1.13 ± 0.07	4	$NaClO_4$
$[SnI_3]^- = Sn^{2+} + 3I^-$, [45]	– 2.13 ± 0.03	4	$NaClO_4$
$[SnI_4]^{2-} = Sn^{2+} + 4I^-$, [45]	– 2.30 ± 0.05	4	$NaClO_4$
$[SnI_6]^{4-} = Sn^{2+} + 6I^-$, [45]	– 2.60 ± 0.04	4	$NaClO_4$
$[SnI_8]^{6-} = Sn^{2+} + 8I^-$, [45]	– 2.08 ± 0.04	4	$NaClO_4$
$Sn^{2+} + [HPO_4]^{2-} = SnHPO_4$, [33]	– 7.71	0.2	$NaClO_4$
$Sn^{2+} + [PO_4]^{3-} = [SnPO_4]^-$, [33]	– 18	0	$NaClO_4$
$Sn^{2+} + [HPO_4]^{2-} = SnHPO_4$, [33]	– 9.5	0	$NaClO_4$
$Sn^{2+} + [H_2PO_4]^- = [SnH_2PO_4]^+$, [33]	– 2.8	0	$NaClO_4$

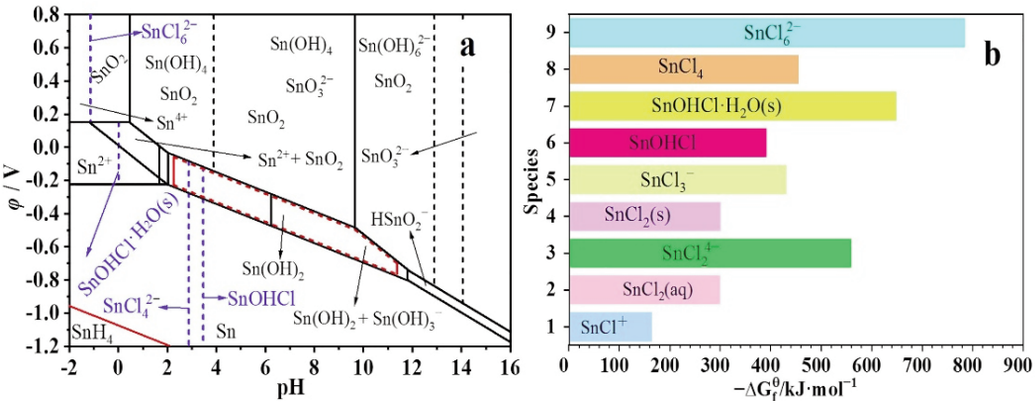

Figure 4. ***a*** *At 298 K, φ-pH diagrams for Sn/H_2O-Cl system at the dissolved Sn activity of 10^{-3}, chloride ions activity of 1, and p[SnH_4(g)] = 1. The Sn species data were retrieved from the reference [27, 33-36, 42, 44, 47-57, 63],* ***b*** *Schematic illustration of the selected ΔG_f^Θ for Sn/H_2O-Cl system at 298 K. The Sn species data were retrieved from the reference [27]*

systems. However, thermodynamic data of Sn/H_2O system commonly focus on 298 K. It is necessary to obtain the thermodynamic data of Sn/H_2O system for Sn development at a high temperature.

This section focuses on the relationship of the potential, pH value, and equilibrium at an elevated temperature for Sn/H_2O system. The standard molar free energy of formation (G_f^Θ / kJ·mol^{-1}) for the selected Sn compounds at 373 K and 550 K is shown in Figure 5, which thermodynamic data are obtained from the reported literature [64].

As shown in Table 3, redox potentials were in conformity with the Nernst equation, and the pH value was in conformity with K^Θ and ΔG_f^Θ.

The Sn species in an aqueous solution are extremely sensitive to temperature. Figures 6a and 6b show the φ-pH diagram for activity of dissolved Sn of 1, 10^{-3}, and 10^{-6} at 373 K and 550 K, respectively. It indicated that the diagrams at 373 K and 550 K were in conformity with the following: (1) The stability fields of Sn species shifted to the lower pH location with increasing temperature; (2) The stability fields of the SnO_2 obviously increased with increasing temperature; and (3) The stability fields of the metallic Sn in an aqueous solution increased with increasing temperature.

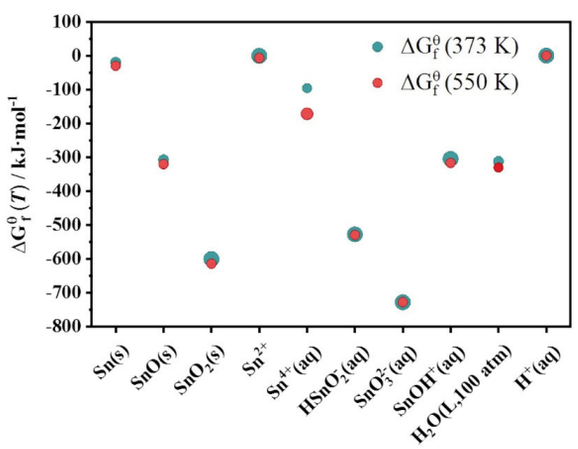

Figure 5. *Schematic illustration of the selected ΔG_f^Θ for Sn/H_2O system at 373 K and 550 K. The Sn species data were retrieved from the reference [64]*

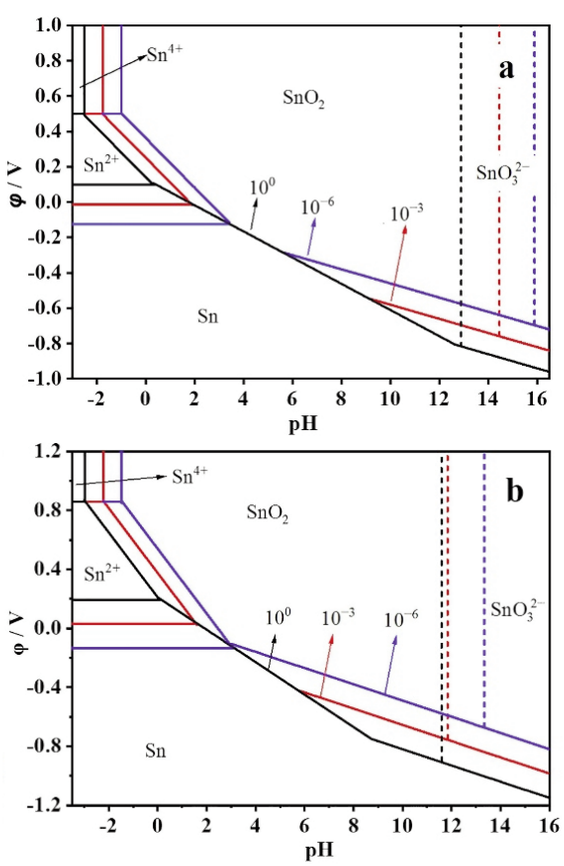

Figure 6. *φ-pH diagrams for Sn/H_2O system under the activity of dissolved Sn of 1, 10^{-3}, and 10^{-6} at a 373 K and b 550 K. The Sn species data were retrieved from the reference [34, 47-50, 55-57]*

Table 3. *The reaction equilibrium for Sn/H_2O system at 373 K and 550 K*

Equilibrium [Ref.]	Temp./K	φ /V or pH
$Sn^{2+} + 2e = Sn$, [34,48-50]	373	$\varphi = 0.1 + 0.037\log\alpha_{(Sn^{2+})}$
	550	$\varphi = 0.19 + 0.055\log\alpha_{(Sn^{2+})}$
$Sn^{4+} + 2e = Sn^{2+}$, [34,48]	373	$\varphi = 0.5 + 0.037\log(\alpha_{(Sn^{4+})}/\alpha_{(Sn^{2+})})$
	550	$\varphi = 0.86 + 0.055\log(\alpha_{(Sn^{4+})}/\alpha_{(Sn^{2+})})$
$SnO + 2H^+ = Sn^{2+} + H_2O$, [34,47]	373	$pH = 0.42 - 0.5\log\alpha_{(Sn^{2+})}$
	550	$pH = 0.16 - 0.5\log\alpha_{(Sn^{2+})}$
$SnO_2 + 4H^+ = Sn^{4+} + 2H_2O$, [34]	373	$pH = -2.51 - 0.25\log\alpha_{(Sn^{4+})}$
	550	$pH = -2.97 - 0.25\log\alpha_{(Sn^{4+})}$
$[HSnO_2]^- + H^+ = SnO + H_2O$, [34,47,50,55]	373	$pH = 12.91 + \log\alpha_{[HSnO_2]^-}$
	550	$pH = 11.6 + \log\alpha_{[HSnO_2]^-}$
$SnO + 2H^+ + 2e = Sn + H_2O$, [34]	373	$\varphi = 0.13 - 0.0741pH$
	550	$\varphi = 0.21 - 0.11pH$
$[HSnO_2]^- + 3H^+ + 2e = Sn + 2H_2O$, [34]	373	$\varphi = 0.61 - 0.11pH + 0.037\log\alpha_{[HSnO2]^-}$
	550	$\varphi = 0.84 - 0.16pH + 0.055\log\alpha_{[HSnO2]^-}$
$SnO_2 + 4H^+ + 2e = Sn^{2+} + 2H_2O$, [34]	373	$\varphi = 0.13 - 0.15pH - 0.037\log\alpha_{(Sn^{2+})}$
	550	$\varphi = 0.21 - 0.22pH - 0.055\log\alpha_{(Sn^{2+})}$
$[SnO_3]^{2-} + 3H^+ + 2e = [HSnO_2]^- + H_2O$, [34]	373	$\varphi = 0.58 - 0.11pH + 0.037\log(\alpha_{[SnO_3]^{2-}}/\alpha_{[HSnO_2]^-})$
	550	$\varphi = 0.69 - 0.16pH + 0.055\log(\alpha_{[SnO_3]^{2-}}/\alpha_{[HSnO_2]^-})$
$[SnO_3]^{2-} + 2H^+ = SnO_2 + H_2O$, [34]	373	$pH = 12.97 + 0.5\log\alpha_{[SnO_3]^{2-}}$
	550	$pH = 10.25 + 0.5\log\alpha_{[SnO_3]^{2-}}$
$SnOH^+ + H^+ = Sn^{2+} + H_2O$, [55-57]	373	$pH = 1.17 - \log(\alpha_{(Sn^{2+})}/\alpha_{Sn(OH)^+})$
	550	$pH = 0.64 - \log(\alpha_{(Sn^{2+})}/\alpha_{Sn(OH)^+})$
$[SnO_3]^{2-} + 6H^+ = Sn^{4+} + 3H_2O$, [55]	373	$pH = 2.65 - 0.17\log(\alpha_{(Sn^{4+})}/\alpha_{[SnO_3]^{2-}})$
	550	$pH = 1.44 - 0.17\log(\alpha_{(Sn^{4+})}/\alpha_{[SnO_3]^{2-}})$

Although the φ-pH diagram for Sn/H_2O system has been extensively researched in past decades, the chemical reaction condition and reaction rate of Sn species cannot be accurately reflected by the previous data. Besides, they cannot be used to describe the thermodynamic properties of Sn alloys. They only describe the thermodynamic behavior of Sn in an acid or base solution and refer to Sn compounds in a system with a certain potential [65]. Despite great progresses in the study of Sn/H_2O system, the reported thermodynamic behavior of Sn and its compounds is inconsistent, and clarifying the thermodynamic behavior of Sn/H_2O systems remains a challenge [42].

4. Sn/H_2O potential-pH diagram application

The φ-pH diagram for Sn/H_2O system has been widely used to evaluate the stability conditions (e.g., the redox potential and the pH value) for metallic Sn and Sn-based products in an aqueous system [65]. In other words, it is used to determine the thermodynamic behavior of Sn species in an aqueous solution [66].

4.1. Corrosion and Passivation

Sn-based materials have been used in many fields because of its good resistance to corrosion. In recent years, due to its non-toxicity property, Sn-based materials have been employed in the metal working industry to replace hazardous metals. They are also widely used in the corrosion inhibiter contacting with an aqueous solution, such as building materials and food packaging field.

The corrosion resistance of Sn is attributed to a thin protective layer of Sn oxide, and the φ-pH diagram can provide thermodynamic information for the passivation layer [67-68]. Figure 3 shows the oxide layer of Sn consisted of $Sn(OH)_4$ or SnO_2 under the condition of pH = 1 ~ 12. In previous studies, the ratio between Sn-OH bond and Sn-O-Sn bond in the

protective layer increased with increasing the pH value. Meanwhile, the protective layer contained a large amount of lattice water in a system with pH > 12.5, indicating that the layer was unstable at a higher pH value [69].

The φ-pH diagram of Sn/H_2O system showed that in a triangular corrosion field, the lower the triangular vertex was, the more easily the surface of metallic Sn was oxidized or passivated [44]. The passivated area of Sn metal was located below the stability fields (the line b) of water because the apex of triangle in triangular corrosion field in Figure 1 and Figure 3 were lower than the line b. This meant that the passivation of metallic Sn was spontaneous.

4.2. Sn Hydrometallurgy

The process of electrorefining, leaching, purification, and deposition is of essential importance for the hydrometallurgy [70]. Fortunately, the φ-pH diagram for Sn/H_2O system can provide the thermodynamic data of the hydrometallurgy. Though, for the analysis of the position of Sn species in the φ-pH diagram, the operating conditions of the hydrometallurgy of were optimized [71, 72]. Additionally, as shown in Figure 7, the φ-pH diagram for Sn/H_2O system provided a theoretical guidance to the Sn electrorefining [73].

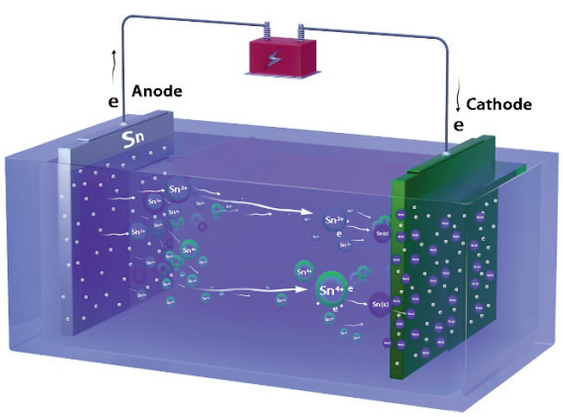

Figure 7. *Schematic diagram of the Sn electrorefining: Metallic Sn is dissolved from the anode and deposited on the cathode*

Taking the extraction in Sn/H_2O system as an example, target metals were leached from an ore in an aqueous solution. The thermochemical behavior can be solved by a φ-pH diagram for Sn/H_2O system, which can provide a way to judge or predict the components and equilibrium of the chemical reaction.

4.3. Electrochemical engineering

Halogen solution, sulfate solution, methyl sulfonate solution, and other organic acid ion solutions are widely applied in the Sn-electrochemical engineering of electroplating and the electrochemical synthesis. Normally, the influence of the redox potential and the pH value on Sn behavior in an aqueous solution cannot be ignored, particularly the electrochemical engineering. As shown in Figure 8, Tannin oxalate (SnC_2O_4) was prepared by the electrochemical method. The thermodynamic behavior of Sn could be determined by the φ-pH diagram of Sn/H_2O system [37].

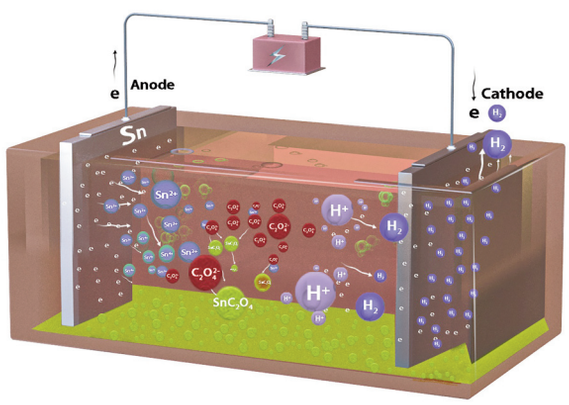

Figure 8. *Schematic diagram of SnC_2O_4 prepared by an electrochemical method in an aqueous solution with $[C_2O_4]^{2-}$ ions. Metal is dissolved at the anode and then reacts with $[C_2O_4]^{2-}$ in an electrolyte to form SnC_2O_4*

Additionally, the φ-pH diagram for Sn/H_2O system provided a reliable theoretical guidance to optimize pH value and the selection of stabilizer in Sn plating fields, and furthermore predict the possibility of Sn co-plating with other metals. The Sn electroplating thermodynamics in Sn/H_2O system can be represented by the equation of $Sn^{2+} + 2e = Sn$, in which the direction and equilibrium of the reaction depended on the redox potential, the logarithm value of Sn^{2+} activities, and the pH value.

Previously, most commercial Sn compounds were synthesized by hydrothermal process, and inorganic Sn compounds such as stannic oxide, stannous oxide, and stannous oxalate were widely used as electrode materials for lithium-ion and sodium-ion batteries. In principle, the φ-pH diagram can provide hydrothermal information to optimize process conditions and to get the desired products [74].

5. Conclusions and perspective

In this paper, the potential-pH diagram for Sn/H_2O system was employed to explore the thermodynamic behavior of Sn species in an aqueous solution. The conditions of Sn species stabilization can clearly be displayed by the potential-pH diagrams. The φ-pH

diagrams of Sn/H_2O system at different conditions (T = 298 K, 373 K, and 550 K, $\alpha_{(Sn)}$ = 1, 10^{-1}, 10^{-3}, and 10^{-6}) and the diagram of Sn/H_2O-Cl system at 298 K provided the thermodynamic data of Sn species in Sn/H_2O system. The relationship of Sn species, the potential, and pH was studied. The metallic Sn was unstable at a redox potential of about 2.02 V. Moreover, Sn(II) compound was Sn^{2+}, $SnOH^+$, $Sn(OH)_2$, $[HSnO_2]^-$, and $[Sn(OH)_3]^-$. The Sn(IV) compounds at the higher redox potential in Sn/H_2O system were $SnO_2(s)$, $Sn(OH)_4$, $[SnO_3]^{2-}$, and $[Sn(OH)_6]^{2-}$. However, Sn(IV) compounds converted to $SnOHCl{\cdot}H_2O(s)$ at pH < 1 and to $[SnCl_4]^{2-}$ at pH ≈ 3 in Sn/H_2O-Cl system. Additionally, the information on the application of φ-pH diagrams for optimizing the production processes was overviewed, particularly in the corrosion and passivation, hydrometallurgy, and electrochemical engineering. In general, thermodynamics played an important role in Sn/H_2O system, and potential-pH diagrams were essential tools for the productive process and the application of Sn. For this reason, the potential-pH diagram was used to interpret thermodynamic behavior of Sn species in Sn/H_2O systems of engineering process.

Acknowledgment

This work is financially supported by the National Natural Science Foundation of China (12175089), the National Key Research and Development Program of China (No. 2019YFC1907900), the Key research and development program of Yunnan Province (202103AF140006, 202103AM140003), the Applied Basic Research Programs of Yunnan Provincial Science and Technology Department (202001AW070004), and the Freely Exploring Fund for Academicians in Yunnan Province (202025AA160008).

Author's contributions

D.R. Yang: conceptualization, validation, writing-original draft. Z.L. Wu: methodology, writing-review. K. Ren: methodology, investigation, validation. P. Dong: investigation, validation. D. Zhang: validation, writing-review & editing. B. Yang: formal analysis, supervision, F. Liang: conceptualization, project administration, visualization, writing-review & supervision.

Data availability

The study did not report any data.

Conflict of Interest

The authors claim that they have no conflicts of interest.

References

[1] E.A.Ostrakhovitch, in Handbook on the toxicology of metals (Fourth Edition), Academic press, San Diego, 2015, 1241-1285.

[2] M.S.B.Silva, R.A.C.Melo, A. L.Lopes-Moriyama, C.P.Souza, Electrochemical extraction of tin and copper from acid leachate of printed circuit boards using copper electrodes, Journal of Environmental Management, 246 (2019) 410-417. https://doi.org/10.1016/j.jenvman.2019.06.009

[3] B. El Ibrahimi, A. Jmiai, K. El Mouaden, A. Baddouh, S. El Issami, L. Bazzi, M. Hilali, Effect of solution's pH and molecular structure of three linear α-amino acids on the corrosion of tin in salt solution: A combined experimental and theoretical approach, Journal of Molecular Structure, 1196 (072) (2019) 105-118. https://doi.org/10.1016/j.molstruc.2019.06.072

[4] M. Gielen, Tin chemistry: fundamentals, frontiers, and applications, John Wiley & Sons, Hoboken, 2008, 1-279.

[5] R.W. Revie, H.H. Uhlig, Corrosion and corrosion control, John Wiley & Sons, Inc, Hoboken, 2008, 43-51.

[6] Z. Wang, X. Guo, J. Montoya, J.K. Nørskov, Predicting aqueous stability of solid with computed Pourbaix diagram using SCAN functional, NPJ Computational Materials, 6(1) (2020) 160. https://doi.org/10.1038/s41524-020-00430-3

[7] J. Fu, X. Jiang, W. Han, Z. Cao, Enhancing the cycling stability of transition-metal-oxide-based electrochemical electrode via Pourbaix diagram engineering, Energy Storage Mate, 42 (2021) 252-258. https://doi.org/10.1016/j.ensm.2021.07.037

[8] E.D. Verink, Simplified procedure for constructing Pourbaix diagrams, Uhlig's corrosion handbook, 7(2011) pages 111-124. https://doi.org/10.1002/9780470872864.ch7

[9] K. Wang, J. Han, A.Y. Gerard, J.R. Scully, B.C. Zhou, Potential-pH diagrams considering complex oxide solution phases for understanding aqueous corrosion of multiprincipal element alloys, NPJ Materials Degradation, 4(1) (2020) 35. https://doi.org/10.1038/s41529-020-00141-6

[10] L.L. Pesterfield, J.B. Maddox, M.S. Crocker, G.K. Schweitzer, Pourbaix (E-pH-M) diagrams in three dimensions, Journal of Chemical Education, 89(7) (2012) 891-899. https://doi.org/10.1021/ed200423

[11] P. Pedeferri, Corrosion science and engineering, Springer, Cham, 2018, 57-72.

[12] M.I. Nave, K.G. Kornev, Complexity of products of tungsten corrosion: comparison of the 3D Pourbaix diagrams with the experimental data, Metallurgical and Materials Transactions A, 48(3) (2017) 1414-1424. https://doi.org/10.1007/s11661-016-3888-6

[13] W.G. Cook, R.P. Olive, Pourbaix diagrams for chromium, aluminum and titanium extended to high-subcritical and low-supercritical conditions, Corrosion Science, 58 (2012) 291-298. https://doi.org/10.1016/j.corsci.2012.02.002

[14] P.A. Nikolaychuk, The third dimension in Pourbaix diagrams: A further extension, Journal of Chemical Education, 91(5) (2014) 763-765. https://doi.org/10.1021/ed400735g

[15] J. Barthel, R. Deiss, The limits of the Pourbaix diagram in the interpretation of the kinetics of corrosion and cathodic protection of underground pipelines, Materials and Corrosion, 72(3) (2021) 434-445. https://doi.org/10.1002/maco.202011977

[16] W.T. Thompson, M.H. Kay, C.W. Bale, A.D. Pelton, Pourbaix diagrams for multielement systems, Uhlig's Corrosion Handbook, 3(2011) 103-109. https://doi.org/10.1002/9780470872864.ch8

[17] L.N. Maskaeva, E.A. Fedorova, R.A. Yusupov, V.F. Markov, Calculating equilrim constants in the $SnCl_2$-H_2O-NaOH system according to potentiometric titration data, Russian Journal of Physical Chemistry A, 92(5) (2018) 1025-1031. https://doi.org/10.1134/S0036024418050230

[18] J.K. Fink, Physical chemistry in depth, Springer, Berlin, 2009, p. 111-143.

[19] N. Perez, Electrochemistry and corrosion science, Springer, Cham, 2016, 1-23. https://doi.org/10.1007/978-3-319-24847-9_1

[20] C.E. Boyd, Physical properties of water, Water quality: an Introduction, (2020) 1-19. https://doi.org/10.1007/978-3-319-17446-4_1

[21] M. Soustelle, Ionic and electrochemical equilibria, John Wiley & Sons, 6(2016) 135-158. https://doi.org/10.1002/9781119178606.ch

[22] W. Hinrichs, S. Dreijer-van der Glas, Practical pharmaceutics, Springer, Cham, 2015, 357-382.

[23] E.S. Rountree, B.D. McCarthy, J.L. Dempsey, Decoding proton-coupled electron transfer with potential-pK_a diagrams: applications to catalysis, Inorganic Chemistry, 58(10) (2019) 6647-6658. https://doi.org/10.1021/acs.inorgchem.8b03368

[24] W. H.Casey, Oxidation-reduction reactions and Eh-pH (Pourbaix) diagrams, Encyclopedia of Geochemistry, 10(2017) 1-6. https://doi.org/10.1007/978-3-319-39193-9_21-1

[25] M.A. Rizvi, Y. Dangat, T. Shams, K.Z. Khan, Complexation key to a pH locked redox reaction, Journal of Chemical Education, 93(2)(2016) 355-361. https://doi.org/10.1021/acs.jchemed.5b00499

[26] N.N. Greenwood, A. Earshaw, Chemistry of the Elements (Second edition), University of Leeds, Leed, 1997, 367-405.

[27] C.I. House, G.H. Kelsall, Potential-pH diagrams for the Sn/H_2O-Cl system, Electrochim Acta, 29(10) (1984) 1459-1464.

https://doi.org/10.1016/0013- 4686(84)87028-0

[28] W.M. White, Encyclopedia of geochemistry, Springer, Cham, 2018, 1443-1445.

[29] P.J. Smith, Chemistry of Tin, Springer, Dordrecht, 1998, 1-289.

[30] P. Gutta, R. Hoffmann, Unusual geometries and questions of oxidation state in potential Sn(III) chemistry, Inorganic Chemistry, 42(25) (2003) 8161-8170. https://doi.org/10.1021/ic034493v

[31] É.G. Bajnóczi, E. Czeglédi, E. Kuzmann, Z. Homonnay, S. Bálint, G. Dombi, I. Persson, Speciation and structure of tin(II) in hyper-alkaline aqueous solution, Dalton Transactions, 43(48) (2014) 17971-17979.

https://doi.org/10.1039/C4DT02706J

[32] O. Davies, D.W.J. Gill, Tin. Oxford Research Encyclopedia of Classics, Oxford, 2016.

https://doi.org/10.1093/acrefore/9780199381135.013.6475

[33] M. Drogowska, L. Brossard, H. Menard, Dissolution of tin in the presence of Cl^- ions at pH 4, Journal of Applied Electrochemistry, 19(2) (1989) 231-238. https://doi.org/10.1007/BF01062306

[34] M. Pourbaix, Atlas of electrochemical equilibria in aqueous solutions, Corrosion Science, 10 (1966) 343. https://doi.org/10.1016/0022-0728(67)80059-7

[35] J. Kragten, The complexometry of tin(IV), Talanta, 22(6) (1975) 505-510. https://doi.org/10.1016/0039-9140(75)80043-9

[36] S.N. Begum, A. Basha, V.S. Muralidharan, C.W. Lee, Electrochemical behaviour of tin in alkali solutions containing halides, Materials Chemistry and Physics, 132(2-3) (2012) 1048-1052. https://doi.org/10.1016/j.matchemphys.2011.12.063

[37] R.M. Cigala, F. Crea, C. De Stefano, G. Lando, D. Milea, S. Sammartano, The inorganic speciation of tin(II) in aqueous solution, Geochimica et Cosmochimica Acta, 87 (2012) 1-20. https://doi.org/10.1016/j.gca.2012.03.029

[38] A.M.S. El Din, F.M.A. El Wahab, On the anodic passivity of tin in alkaline solutions, Electrochimica Acta, 9(7) (1964) 883-896. https://doi.org/10.1016/0013- 4686(64)85039-9

[39] P. Pedeferri, Corrosion science and engineering, Springer, Cham, 2018, 1-102.

[40] V.I. Lakshmanan, M.A. Halim, S. Vijayan, Innovative process development in metallurgical industry, Springer, Cham, 2016, 91-108.

[41] M.V. Cases, Á.I. López-Lorente, M.Á. López-Jiménez, Foundations of analytical chemistry, Springer-Verlag, Berlin, 2018, 3-52.

[42] C. Lefrou, P. Fabry, J.C. Poignet, Electrochemistry, Springer, Berlin, 2012, 119-168.

[43] L. Pogliani, Construction and usefulness of the Pourbaix E-pH diagrams, Chemistry and Industrial Techniques for Chemical Engineers, (2020) 3-19. https://doi.org/10.1201/9780429286674-2

[44] E.D. Verink, Simplified procedure for constructing Pourbaix diagrams, Uhlig's Corrosion Handbook, 7(2011) 111-124. http://corrosionjournal.org/doi/abs/10.5006/0010-9312-23.12.371

[45] D.W. Barnum, Potential-pH diagrams, Journal of Chemical Education, 59(10)(1982) 809. https://doi.org/10.1021/ed059p809

[46] O. Toshiaki, Potential-pH diagram for understanding the metallic corrosion and its limitation, Journal of the Surface Finishing Society of Japan, 64(2) (2013) 99-103. https://doi.org/10.4139/sfj.64.99

[47] A.B. Garrett, R.E. Heiks, Equilibria in the stannous oxide-sodium hydroxide and in the stannous oxide-hydrochloric acid systems at 25 °C. Analysis of dilute solutions of stannous Tin, Journal of the American Chemical Society, 63(2) (1941) 562-567. https://doi.org/10.1021/ja01847a058

[48] N.A. Hampson, N.E. Spencer, Anodic behaviour of Tin in potassium hydroxide solution, British Corrosion Journal, 3(1) (1968) 1-6. https://doi.org/10.1179/000705968798326523

[49] W. Jun, P. Yun, E. Lee, Leaching behavior of tin from Sn-Fe alloys in sodium hydroxide solutions, Hydrometallurgy, 73(1-2) (2004) 71-80.

https://doi.org/10.1016/j.hydromet.2003.08.002

[50] L.S.Y. Lee, F. Lawson, The leaching rate of tin metal in oxygenated sodium hydroxide solutions, Hydrometallurgy, 23(1) (1989) 23-35. https://doi.org/10.1016/0304-386X(89)90015-7

[51] B.N. Stirrup, N.A. Hampson, Anodic passivation of tin in sodium hydroxide solutions, Journal of Electroanalytical Chemistry and Interfacial Electrochemistry, 67(1) (1976) 45-56. https://doi.org/10.1016/S0022-0728(76)80063-0

[52] E.E.F. El-Sherbini, Perchlorate pitting corrosion of tin in Na_2CO_3 solutions and effect of some inorganic inhibitors, Corrosion Science, 48(5) (2006) 1093-1105. https://doi.org/10.1016/j.corsci.2005.05.013

[53] H.H. Hassan, S.S. Abd El Rehim, N.F. Mohamed, Role of ClO_4^- in breakdown of tin passivity in NaOH solutions, Corrosion Science, 44(1)(2002) 37-47. https://doi.org/10.1016/S0010-938X(01)00040-3

[54] P.E. Alvarez, S.B. Ribotta, M.E. Folquer, C.A. Gervasi, J.R. Vilche, Potentiodynamic behaviour of tin in different buffer solutions, Corrosion Science, 44(1) (2002) 49-65. https://doi.org/10.1016/S0010-938X(01)00032-4

[55] F. Séby, M. Potin-Gautier, E. Giffaut, O.F.X. Donard, A critical review of thermodynamic data for inorganic tin species, Geochimica et Cosmochimica Acta, 65(18) (2001) 3041-3053. https://doi.org/10.1016/S0016-7037(01)00645-7

[56] M. Pettine, F.J. Millero, G. Macchi, Hydrolysis of tin(II) in aqueous solutions, Analytical Chemistry, 53(7) (1981) 1039-1043.

https://doi.org/10.1021/ac00230a027

[57] R.S. Tobias, Studies on the hydrolysis of metal ion, Acta Chemica Scandinavica, 12(2) (1958) 198-223. https://doi.org/10.3891/acta.chem.scand.12-0198

[58] S. Lyon, in Shreir's corrosion (Tony JAR. Ed.), Elsevier, Oxford, 2010, p. 2068-2077.

[59] T. Gajda, P. Sipos, H. Gamsjäger, The standard redox potential of the Sn^{4+}/Sn^{2+} couple revisited, Monatshefte für Chemie-Chemical Monthly, 140(11) (2009) 1293-1303. https://doi.org/10.1007/s00706-009-0188-5

[60] É.G. Bajnóczi, B. Bohner, E. Czeglédi, E. Kuzmann, Z. Homonnay, A. Lengyel, P. Sipos, On the lack of capillary Mössbauer spectroscopic effect for Sn^{II}-containing aqueous solutions trapped in corning Vycor "thirsty" glass, Journal of Radioanalytical and Nuclear Chemistry, 302(1)(2014) 695-700. https://doi.org/10.1007/s10967-014-3247-2

[61] B.A.Addia, E.A.Addia, M.Hamdani, The effects of chloride and sulphate ions on the electrochemical behaviour of tin in aqueous solutions, Portugaliae Electrochimica CAta, 36(1)(2018) 11-22. https://doi.org/10.4152/pea.201801011

[62] D. Wang, R. Mathur, W. Powell, W.P owell, L. Godfrey, Y. Zheng, Experimental evidence for fractionation of tin chlorides by redox and vapor mechanisms, Geochimica et Cosmochimica Acta, 250(2019) 209-218. https://doi.org/10.1016/j.gca.2019.02.022

[63] T. Wang, J.X. She, K. Yin, K. Wang, Y.J. Zhang, X.C. Lu, X.D. Liu, W. Li, Sn (II) chloride speciation and equilibrium Sn isotope fractionation under hydrothermal conditions: A first principles study, Geochimica et Cosmochimica Acta, 300(2021) 25-43. https://doi.org/10.1016/j.gca.2021.02.023

[64] M.H. Kaye, W.T. Thompson, Computation of Pourbaix diagrams at elevated temperature, Uhlig's corrosion handbook, 3(2011) 111-122. https://doi.org/10.1002/9780470872864.ch9

[65] A.M. Patel, J.K. Nørskov, K.A. Persson, J.H. Montoya, Efficient Pourbaix diagrams of many-element compounds, Physical Chemistry Chemical Physics, 21(45)(2019) 25323-25327 3. https://doi.org/10.1039/C9CP04799A

[66] H.H. Huang, The Eh-pH diagram and its advances, Metals, 6(1) (2016) 23. https://doi.org/10.3390/met6010023

[67] E.E.F. El-Sherbini, S.M. Abd-El-Wahab, M.A. Amin, M.A. Deyab, Electrochemical behavior of tin in sodium borate solutions and the effect of halide ions and some inorganic inhibitors, Corrosion Science, 48(8) (2006) 1885-1898. https://doi.org/10.1016/j.corsci.2005.08.002

[68] B.X. Huang, P. Tornatore, Y.S. Li, IR and Raman spectroelectrochemical studies of corrosion films on tin, Electrochimica Acta, 46(5) (2019) 671-679. https://doi.org/10.1016/S0013-4686(00)00660-5

[69] C.A. Moina, G.O. Ybarra, Study of passive films formed on Sn in the 7-14 pH range, Journal of Electroanalytical Chemistry, 504(2) (2001) 175-183. https://doi.org/10.1016/S0022- 0728(01)00432-6

[70] J.W. Evans, L.C. De Jonghe, Hydrometallurgy and electrometallurgy, The Production and Processing of Inorganic Materials, (2016) 281-320. https://doi.org/10.1007/978-3-319-48163-0_9

[71] Z.H. Cao, B.Z. Ma, C.Y. Wang, Y.Q. Chen, B. Liu, P. Xing, W.J. Zhang, E-pH diagrams for the metal-water system at 150 °C: Thermodynamic analysis and application for extraction and separation of target metals from saprolitic laterite, Minerals Engineering, 152(2020) 106365. https://doi.org/10.1016/j.mineng.2020.106365

[72] D.M. Sherman, K.V. Ragnarsdottir, E.H. Oelkers, C.R. Collins, Speciation of tin (Sn^{2+} and Sn^{4+}) in aqueous Cl solutions from 25 °C to 350 °C: an in situ EXAFS study, Chemical Geology, 167(1-2) (2000) 169-176. https://doi.org/10.1016/S0009- 2541(99)00208-9

[73] B. Zhang, D.C. Liu, H. Xiong, Z.G. Zhou, X. Li, L. Li, B. Yang, X.P. Gu, S.P. Wang, The new method to separate stannum and copper in the process of refining Tin, Materials Science Forum, Trans Tech Publications ltd, 996(2020) 157-164. https://doi.org/10.4028/www.scientific.net/MSF.996.157

[74] B.R. Chen, W. Sun, D.A. Kitchaev, K.H. Stone, R.C. Davis, G. Ceder, M.F. Toney, Kinetic origins of the metastable zone width in the manganese oxide Pourbaix diagram, Journal of Materials Chemistry, 9(12) (2021) 7857-7867. https://doi.org/10.1039/D0TA12533D

SKORAŠNJI NAPREDAK U POZNAVANJU TERMODINAMIČKOG PONAŠANJA KALAJA U VODENOM RASTVORU

D.-R. Yang [a,b], Z.-L. Wu [c,d], K. Ren [a,b], P. Dong [a,b], D. Zhang [a,b *], B. Yang [a,b], F. Liang [a,b *]

[a] Fakultet za metalurško i energetsko inženjerstvo, Univerzitet nauke i tehnologije u Kuenmingu, Kuenming, Kina

[b] Državni inženjerski istraživački centar za vakuumsku metalurgiju, Univerzitet nauke i tehnologije u Kuenmingu, Kuenming, Kina

[c] Fakultet za nauku o materijalima, Univerzitet u Šendđenu, Šendžen, Kina

[d] Zhejiang LAMP Co., Ltd., Vendžou, Kina

Apstrakt

Termodinamičko ponašanje se uveliko koristi za procenu stabilnosti materijala i predviđanje pravca hemijske reakcije pri različitim pH vrednostima, temperaturama, potencijalima i koncentracijama jona. Iako postoje pokušaji istraživanja Sn u sistemu vodenog rastvora (Sn/H_2O) kiseline, alkalija i soli, rezultati koji se ne mogu naći na jednom mestu dovode do neefikasnosti termodinamičke metode u praktičnoj primeni. Ovaj rad daje kratak pregled dijagrama potencijal-pH za sistem Sn/H_2O koji odražava termodinamičko ponašanje Sn u vodenom rastvoru i izdvaja termodinamičke podatke za praktičnu primenu različitih vrsta Sn. Prvo je sagledan odnos termodinamičkog ponašanja, dijagrama potencijal-pH i ravnotežnih odnosa Sn za sistem Sn/H_2O. Pored toga, ispitan je dijagram potencijal-pH za sistem Sn/H_2O na različitim temperaturama (298 K, 373 K i 550 K), aktivnosti rastvorenog Sn (1, 10^{-1}, 10^{-3} i 10^{-6}), kao i dijagram potencijal-pH za različite vrste Sn u vodenom rastvoru hloridiona (Sn/H_2O-Cl). Na kraju je istražena i perspektiva primene dijagrama potencijal-pH za sistem Sn/H_2O pomoću simulacije metalurgije kalaja i praktične primene Sn materijala.

Ključne reči: *Sn/H_2O sistem; Dijagram potencijal-pH; Termodinamičko ponašanje; Redoks potencijal; Ravnoteža*